Fachtagung "Lasermethoden in der Strömungsmesstechnik"
8.–10. September 2009, Erlangen

Stably Stratified Isokinetic Turbulent Mixing Layers: Comparison Of PIV-Measurements And Numerical Calculations

Stabil stratifizierte isokinetische Mischungsschichten: Vergleich zwischen PIV Messungen und CFD-Rechnungen

J. Fokken, R. Kapulla, S. Kuhn , C. Dyck, H.M. Prasser
Labor für Thermohydraulik (LTH), Paul Scherrer Institut, 5232 Villigen, Schweiz

Isokinetische Mischungsschicht, PIV, LES
Isokinetic mixing layers, PIV, LES

Abstract

The turbulent mixing of coolant streams of different temperature and density causes severe temperature fluctuations, which may lead to thermal fatigue in the junctions where mixing occurs. The aging phenomena resulting from thermal fatigue is the reason for an increased interest in measuring and predicting the flow field and turbulent mixing flow patterns evolving downstream of a mixing point. To study the fundamental mixing phenomena, the current co-flow isokinetic water experiments were carried out in a square channel with Reynolds-Numbers covering the range of $Re = 5 \cdot 10^3$ to 10^5 at various relative densities. Particle Image Velocimetry (PIV) was used to measure the velocity field and the results are compared with 3D large-eddy simulations (LES). A very good agreement in shape and magnitude was found for the mean and RMS-velocity field, except for the transverse-velocity component where LES underpredicts the magnitude of the fluctuations. Spatial velocity correlation maps reveal a distinct effect of the density difference on the evolution and decay of orderly structures with downstream distance. It is shown that the correlation maps are in close agreement with the numerical results. The reduced size of these orderly structures in the presence of density differences indicate a corresponding inhibiting effect on the mixing process which requires further analysis and the use of measurement techniques that are capable of resolving the mixing process directly.

1 Introduction

One important issue in the management of aging in nuclear power plants is the monitoring and assessment of thermal fatigue. Thermal fatigue is a mechanism which results in significant degradation of the mechanical properties of a material exposed to cyclic thermal stresses, which superimposes on the mechanical loads. Due to thermal fatigue a component may fail before its design lifetime. Typical components, which are susceptible to thermal fatigue are junctions where two fluids with different temperatures mix. Following the Civaux Unit 1 (F) incident, (Chapuilot et al. 2005), for example, several T-junction experiments (Metzner and Wilke 2005) and (Walker et al. 2009) have been carried out, to study the mechanisms leading to pipe cracks as a result of thermal loading in flow mixing zones. However, there are still difficulties in predicting the location of failure with numerical codes in such mixing zones. The current water mixing experiments in the GEMIX-Facility (**Ge**neric **Mix**ing E**x**periment) are focused on the basic mechanisms of turbulent mixing in the presence of temperature and/or density gradients under isokinetic mixing conditions. The velocity field is studied using Particle Image Velocimetry (PIV) in the current experiments. To measure simultaneously the concentration field, which provides information about the mixing process, Wire-Mesh sensors (WMS) and Wall sensor (WLS) will be used, (Prasser et al. 1998). In a first step, we compare the veloc-

ity information with the corresponding numerical simulations using the commercial CFD-Code Fluent (V6.3).

2 Experiment

The GEMIX facility is designed to investigate the effect of density-differences as well as the effect of viscosity- and temperature-differences on turbulent mixing. The main parts of the facility are pictured in figure 1.

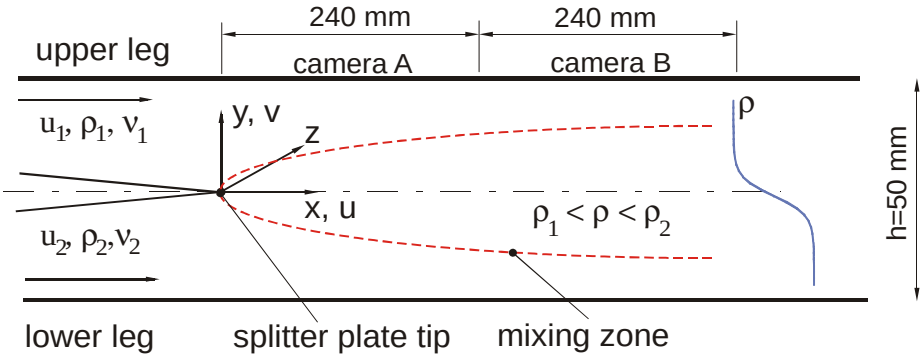

Figure 1: *Schematic of the GEMIX facility.*

The two streams, denoted by lower and upper leg, are initially separated by a splitter plate. In the conditioning section, both streams pass through honeycombs and grids, such that the velocity profiles at the splitter plate tip are flat and free from rotational components. After the tip of the splitter plate both streams interact and form the mixing zone. The water loop driving the test section establishes equal initial velocities for both streams, i.e. isokinetic conditions $u_1{=}u_2{=}u_0$ in the range from 0.1 to 1 m/s . Additionally, the density, ρ, and the kinematic viscosity of both fluid streams, ν, can be adjusted by varying the temperature and adding sucrose to the fluid in one leg to increase the density difference without influencing the electric conductivity. The latter becomes important when additionally working with wire-mesh sensors measuring the conductivity. The GEMIX facility consists of an acrylic glass channel with square cross-section (50x50 mm). The test section is fed from two storage tanks having a volume of 2000 l each. This enables separate conditioning of either stream. The storage capacity allows for experiments upt to 15 min for the highest velocity of $u_0{=}1$ m/s. The loop is open, i.e. the water is purged to the drain after mixing.

Exp. No.	u_0 m/s	T_1 °C	T_2 °C	Re_1 –	Re_2 –	ρ_1 kg/m^3	ρ_2 kg/m^3	$\Delta\rho$ %	Ri –	Sugar cont. c [mass – %]
N109	0.2	50	20	11400	6300	988	998	1	0.125	0
N116	0.2	20	20	6300	6300	988	998	0	0	0
N122	1	20	20	31400	31400	988	998	0	0	0
N131	1	50	20	40500	31400	1055	998	5	0.028	15

Table 1: Experimental program and boundary conditions.

The origin of the coordinate system to describe the flow field is located at the splitter plate tip in the centre of the channel. For the PIV recording we use a DANTEC PIV system consisting of two identical cameras (Kodak MegaPlus ES 1.0, 1016x1008 pixel) and a system hub to run both cameras simultaneously with a maximum recording frequency of 15 Hz. Both cameras are positioned perpendicular to the $x-y$-plane, such that there is a $\approx$100 pixel overlap in the recorded images at x=240 mm downstream of the splitter plate. The laser light sheet generated in the x-y-plane with a New Wave Gemini 200 mJ laser was positioned in the middle of the channel (i.e. z=0). The particle images were analysed with DaVis V7.2 from LaVison using a multi pass, decreasing window size and window shift approach with a final interrogation window size of 12x12 pixel, (Raffel et al. 2007). With one pixel corresponding to 0.25 mm

and using 50 % overlap for the analysis a spatial resolution of 1.5 mm is obtained. Vestosint No2158 irregular shaped seeding particles having a nominal diameter of 21 μm and a density of 1.02 g/cm^3 were injected with a variable speed syringe pump to maintain particle number densities independent of flow rate for all the experiments. For all runs 1024 double-frame, single exposure images were recorded and subsequentially analysed. Parameters for the experiments under consideration were the inlet bulk velocity, u_0, in the range from 0.2 to 1 m/s and the relative density difference, $\Delta\rho$, from 0 to 1 $\%$ between the two legs, Table 1.

3 Results

The use of optical methods for the study of mixing in the presence of strong density gradients is severely challenged by the corresponding variation of refractive index in the mixing region. The mixing zone will distort any light passing through it when there is a difference in the refractive index of the two fluids. The analysis of these blurry images with the classical cross correlation technique was not able to produce reliable velocity fields in the mixing zone, therefore the results from the case with $\Delta\rho$ =5 % will not be included here, see instead (Kapulla et al. 2009). The experimental results for run N116, i.e. for a bulk velocity of u_0=0.2 m/s, were compared with corresponding numerical calculations using 3D large-eddy-simulation (LES). In the LES approach a spatial filter operation is applied which is based on the computational mesh. All scales of the fluid motion which are resolved by the grid are captured directly in the solved equations, only the contribution of the subgrid-scale motions needs to be modeled. Thus the LES approach invokes less modeling compared to RANS models (e.g. $k-\varepsilon-$turbulence model) and is therefore more computational expensive. However, this degree of detail associated with the LES method makes it better suited to address the instantaneous mixing processes and its associated scales; therefore LES was used in this study instead of the classical $k-\varepsilon-$turbulence model. The equations describing turbulent flow are given by the conservation of mass, ρ, and momentum, ρu_i. Applying a spatially uniform filter operation, the conservation of momentum reads (Pope 2000)

$$\frac{\partial\left(\rho\overline{u_i}\right)}{\partial t}+\frac{\partial\left(\rho\overline{u_j u_i}\right)}{\partial x_j}=-\frac{\partial\overline{p}}{\partial x_i}+\mu\frac{\partial^2\rho\overline{u_i}}{\partial x_j\partial x_j}-\frac{\partial\rho\tau_{ij}^R}{\partial x_j}$$

where $\overline{p}$ is the filtered pressure field, and μ denotes the dynamic viscosity of the fluid. LES simulations are performed by using the dynamic Smagorinsky model for the subgrid scales. The unresolved traceless subscale stresses τ_{ij}^R are related to the rate of strain $\overline{S_{ij}}$ of the resolved velocity field by employing the Boussinesq eddy-viscosity concept

$$\tau_{ij}^R-\frac{1}{3}\tau_{kk}\delta_{ij}=-2\nu_T\overline{S_{ij}}$$

The eddy viscosity is defined as

$$\nu_T=\left(C_S\Delta\right)^2\left|\overline{S}\right|$$

where Δ denotes the length scale of the unresolved motion calculated from the volume of the computational cell ΔV

$$\Delta=\sqrt[3]{\Delta V}$$

and $\left|\overline{S}\right|$ is the magnitude of the strain rate defined as

$$\left|\overline{S}\right|=\sqrt{2\overline{S_{ij}S_{ij}}}$$

For the dynamic Smagorinsky model C_S is evaluated from the dynamical procedure (Germano et al. 1991)

$$C_S=-\frac{1}{2}\frac{L_{ij}M_{ij}}{M_{ij}M_{ij}}$$

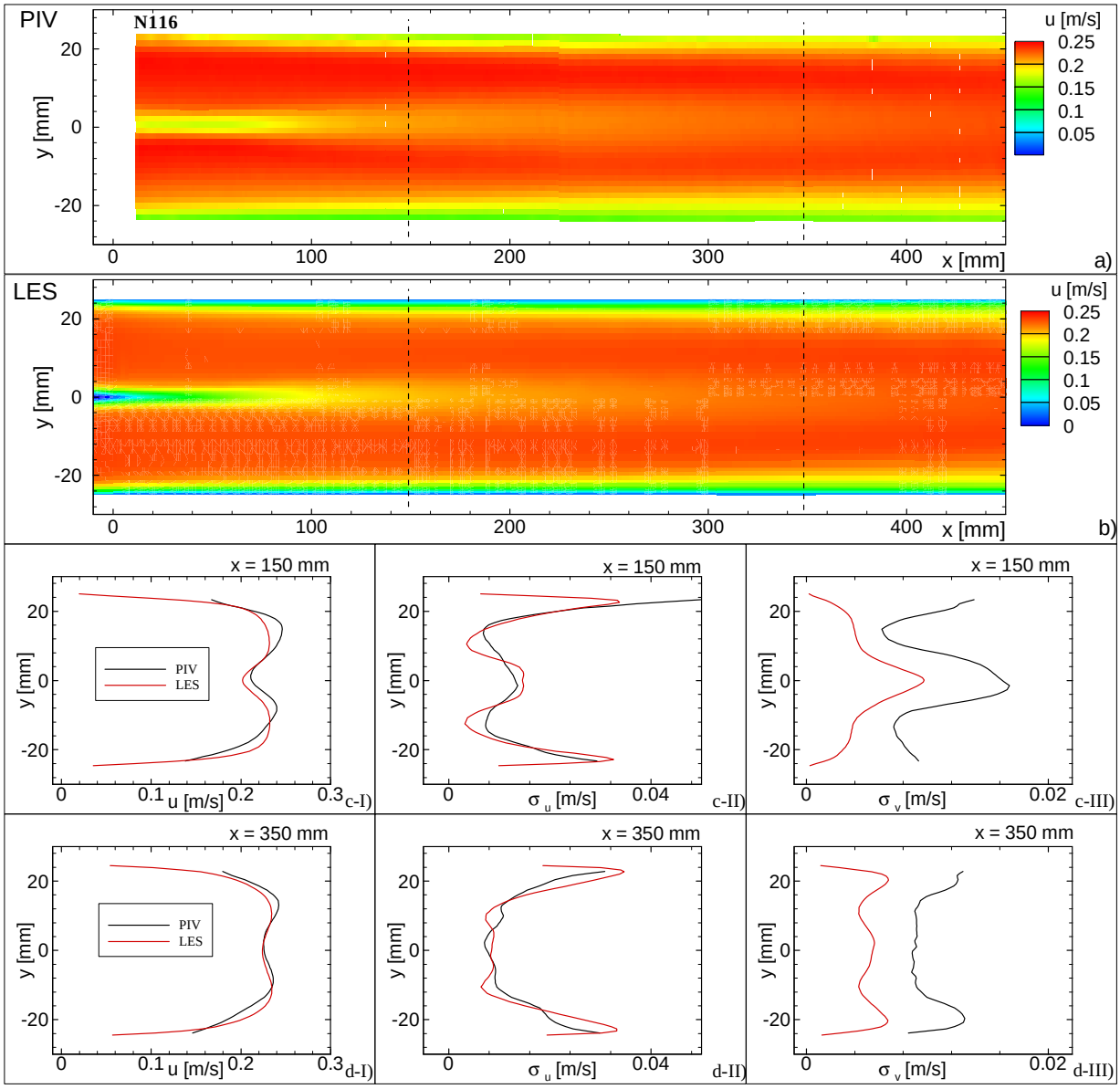

Figure 2: *Comparison of experimental (N116) and numerical results for a bulk velocity of* $u_0 = 0.2$ m/s.

The value of C_S is clipped at zero to avoid backscattering. The dynamic procedure to obtain the Smagorinsky constant ensures correct near wall behaviour of the turbulent viscosity eliminating the necessity to include wall-damping functions. The computations were performed by using the commercial software package FLUENT, which provides a finite-volume based solver accurate to the second order. We computed the case with a velocity of 0.2 m/s in each of the channel inlets without buoyancy effects, i.e. mixing of two water streams with the same density. For this study the channel was discretized with a streamwise length of 0.79 m, starting 0.19 m upstream of the splitter plate tip corresponding to flow conditioning dimensions in the experimental inlet. The hexahedral mesh for this geometry consisted of 1.975 million cells (395 elements in streamwise direction, x, 100 elements in vertical direction, y, and 50 elements in spanwise direction, z). A total of 10 s of flow time (real time) was computed for this case and data for statistics were sampled at a frequency of 4 Hz. The comparison of the experimental and numerical results with a bulk velocity of u_0=0.2 m/s are depicted in Figure 2. The mean velocity component u is compared in Figure 2 a) and b). It is evident that mean velocity profile

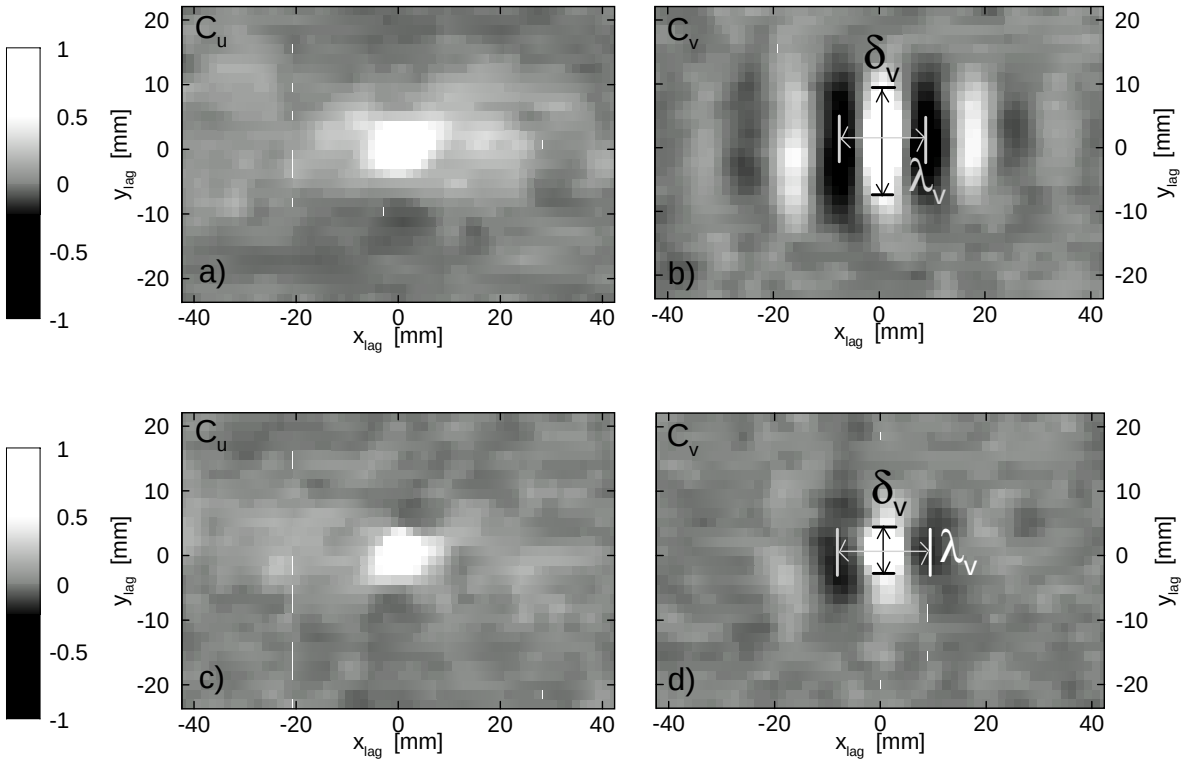

Figure 3: *Correlation map in the mixing zone for a bulk velocity of 0.2 m/s (upper two images, N116) and 1.0 m/s (lower two images, N122) for u' (left two images) and v' (right two images). Images a) and b) run N116 and images c) and d) run N122.*

in the streamwise direction, u, predicted by LES is very similar to the mean velocity profile in the corresponding experiment, except in the region close to the splitter plate (0 <x<100 mm) where the code calculates smaller velocities and the boundary layers which were better resolved by the fine mesh used in the code. To highlight these findings for both the experimental and numerical results, vertical profiles of the mean velocity u, the standard deviation σ_u as well as σ_v were extracted at x=150 mm and 350 mm, respectively. It is found that the experimental mean velocity exhibits an asymmetry in the lower flow profile, Figure 2 c-I) caused by inferior construction of the flow conditioning grids. Future experiments will be performed with a new improved inlet section and a new water loop with more accurate flowmeters. When the standard deviation in σ_u from experiment and LES is compared, the result is also in good agrement for the most part, except near the walls where LES predicts a drop in σ_u as dictated by non-slip boundary conditions but experiments show that σ_u only continues to grow, figure 2 c-II und d-II. This discrepancy is of little significance to the study which is concerned with the mixing process in the center of the channel. When the standard deviation in σ_v from experiment and LES is compared, there is a difference, Figure 2 c-III und d-III. Although the profile shapes are similar, the experiment shows almost twice the σ_v as the LES predicts. This might be caused a) by a redistribution of fluctuations from the v to the w velocity components in the LES calculation or b) by increased measurement errors in the experiment resulting from relatively small particle shifts. This topic requires further investigation.

The correlation concept can be used in fluid mechanics to determine, how strongly flow properties – velocities for the present case – at different spatial locations vary together. The correlation strength can be interpreted as a measure of the information exchange between these locations. The correlation coefficient C at a given point (x_{lag},y_{lag}) in the correlation map is obtained by correlating the velocities at the reference location (x_0, y_0) with the velocities at a nearby location (x_0+x_{lag},y_0+y_{lag}). Using the decomposition U=u+u′ where u denotes mean und

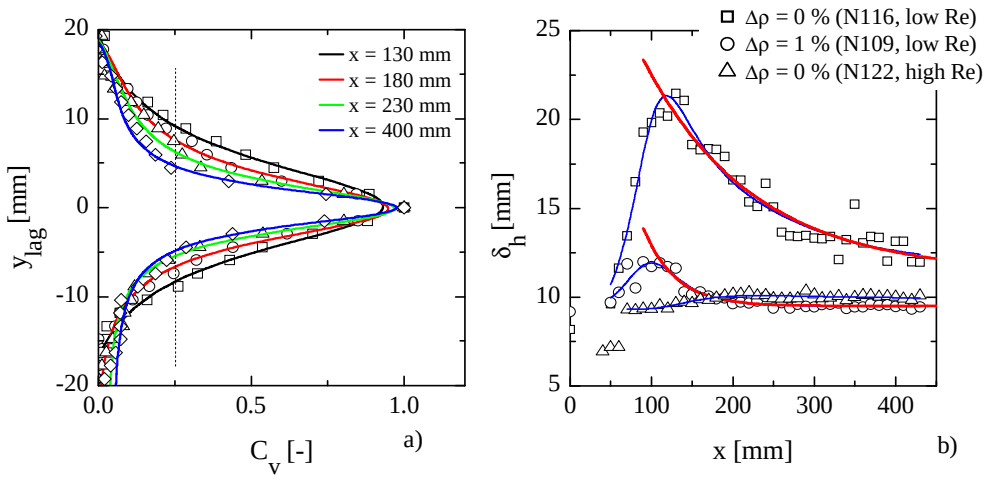

Figure 4: *One dimensional vertical spatial correlations* C_h *at distances x=130, 180, 230 and 400 mm (left, N116) and vertical elongation of the correlation zone as a function of downstream distance with density difference and Re-number as parameter (right N116, N019 and N 122.*

u′ fluctuating components and together with the abbreviations $U_n(x_0,y_0) = U_{n,0}$, $u(x_0,y_0) = u_0$, $U_n(x_0+x_{lag},y_0+y_{lag}) = U_{n,lag}$ and $u(x_0+x_{lag},y_0+y_{lag}) = u_{lag}$ the correlation map can be described with:

$$C_u(x_{lag}, y_{lag}) = \frac{1}{N-1} \frac{\sum_{n=1}^{N} \{[U_{n,0} - u_0] \cdot [U_{n,lag} - u_{lag}]\}}{\sigma_u \{U_0 - u_0\} \cdot \sigma_u \{U_{lag} - u_{lag}\}}$$

Strictly speaking, the equation which was used to calculate the 'correlation coeffients' calculates the normalized covariance which returns C=1 when the velocity fluctuations at both locations are perfectly correlated, i.e. $x_{lag}=y_{lag}=0$; C=0 when the velocity fluctuations are not correlated; and C becomes negative when the velocity fluctuations are inversely correlated. We denote the number of valid vectors with N that exist at both positions (x_0, y_0) and (x_0+x_{lag}, y_0+y_{lag}), and σ_u denotes the standard deviation. Spatial correlation maps are presented for ($x_0=160$, $y_0=0$) for both the u′ and v′ components of the velocity for mixing with low and high Reynolds numbers in figure 3. Irrespective of the Re-number one can observe different bahaviour in the u′ and v′ velocity component. The C_u correlation map shows an almost circular peak around (x_0, y_0) indicating isotropic correlations, while the C_v correlation map shows a very distinct repetition in the x-direction and an pronounced elongation in the y-direction. This indicates a repetitive structure in the v′ velocity component within the mixing zone and contains some additional information about the size, shape, and frequency of these repetitive structures. The size of the circular correlation spot for C_u typically decreases for increasing Re-numbers. The correlation peak height, δ_v see figure 3, can be considered one measure of the orderly structures within the mixing zone since these repetitive structures will be correlated with themselves, but uncorrelated with the free stream outside of the mixing zone. The vertical correlation coefficient profile at $x_{lag}= 0$ (x=160 mm) can be extracted from the C_v correlation map, and compared with corresponding profiles at various distances from the splitter plate tip, figure 4a) which shows a decrease in the correlation zone height δ_v with downstream distance. In order to quantify δ_v a second order polynomial was fit to points of the correlation profile, figure 4 a), above a threshold correlation value of $C_{v,thresh}=0.25$. The zeros of this fit were taken as the height, δ_v, of the v′ correlation zone. The correlation height as a function of downstream distance is presented in figure 4 b). One can distinguish two regimes: One regime where the orderly structures develop (0 mm<x<120 mm) and one regime where the structure size follows an exponential decay law (120 mm<x<400 mm). The size of the structures, however, is much smaller when a stratification is superimposed. For the high Re-number case, figure 4 b) N122,

one finds a weak developing zone and for x>150 mm, δ_v remains almost constant. Similar to figure 4 a), the correlation coefficient C_v can be extracted from figure 3 along a horizontal line y_{lag}=0 (y=0 mm), the results show a periodic repetition with a single dominant wavelength λ_v in figure 5 a). It should be noted that this wavelength was extracted by eye and plotted as a function of downstream distance in figure 5 b). The wavelength increases with downstream distance showing a faster growth for higher Re-numbers. For higher downstream distances it becomes difficult to determin the wavelength accurately since the periodicity becomes less pronounced especially for lower Re-numbers. The experimental and numerical results were

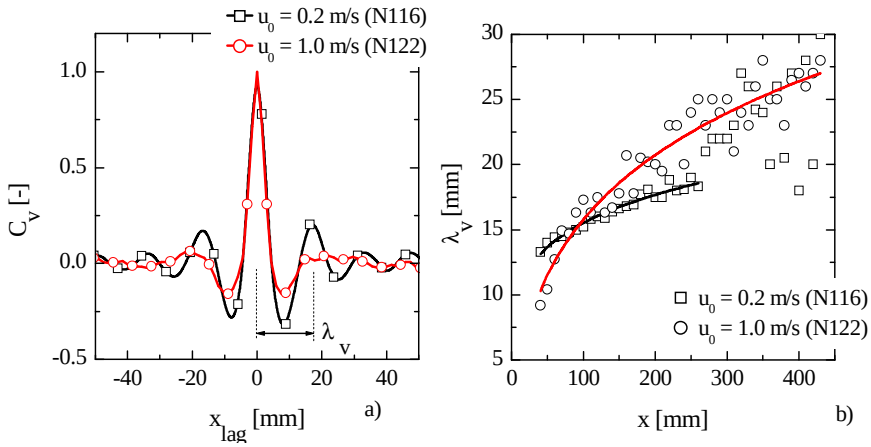

Figure 5: *One dimensional horizontal spatial correlations C_v at distance x=160 (left, N116) and characteristic wavelength λ_v as a function of downstream distance with Re-number as parameter, (right, N116 and N 122).*

also compared using correlation maps. For the numerical result only 1 instantaneous velocity field was available; therefore, in order to obtain enough samples to compute a reasonable correlation map, the correlation had to be computed over a larger area, which was chosen as x=120 mm to x=200 mm. To be consistent with the numerical results a single, randomly chosen instantaneous velocity field was extracted from the experimental results, and the correlation map was computed for the same area (x=120 mm to x=200 mm). A comparison of figure 3 with figure 6 reveals that the basic structure of the correlation map is the same regardless of the size of the area, or the number of frames that the correlation is calculated from. It should be noted, however, that less data result in a noiser correlation map, figure 6 a). Comparison of the experimental and numerical correlation maps shows that LES predicts similar orderly structures in the mixing zone. However, the structures present in the simulation are larger (in both x and y direction) than the experiment. This difference may be an important outcome,

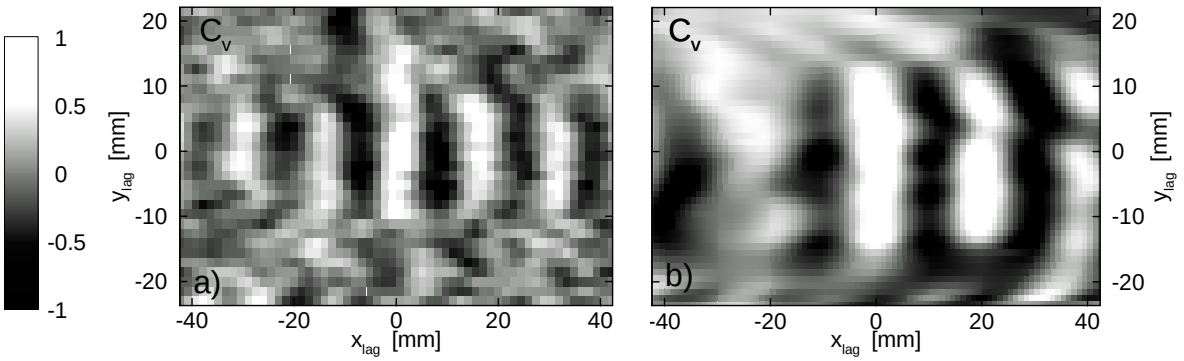

Figure 6: *Experimental (left, N116) and numerical correlation map* C_v.

because the frequency of velocity fluctuations is directly related to the horizontal size of the correlation through the mean velocity u.

4 Summary

To study fundamental mixing phenomena, water experiments were carried out in a square channel with Reynolds-Numbers covering the range of Re=$5 \cdot 10^3$ to 10^5 at various relative densities $\Delta\rho$. After conditioning in the inlet section, two streams with a density difference from 0 to 1% and the same velocity (isokinetic flow) interact and form the mixing zone. The results were compared with corresponding LES calculations. It was shown that mean velocity and velocity fluctuations in main flow direction, u, predicted by LES are in very good agreement with the measurements in both shape and magnitude. The only exception is in the region close to the splitter plate ($0<x<100$) where the code calculates smaller velocities, and in the boundary layers which were better resolved by CFD. The latter discrepancy is of little significance to the study which is concerned with the mixing process in the center of the channel. In the transverse velocity fluctuation, σ_v, there is a discrepancy between experiment and LES. Although the profile shapes are similar, the experiment shows almost twice the σ_v as the LES predicts. Spatial correlation maps C_v revealed the presence of orderly structures in the mixing zone which show reasonable agreement with the numerical results. The height of these structures follows an exponetial decay law with downstream distance.

Acknowledgements

The Authors would like to thank: Nordostschweizerische Kraftwerke AG (NOK) for funding the PhD-Thesis and sponsoring part of the experimental equipment. Wilhelm Bissels (PSI, LTH) for the technical and mechanical support. Dipl.-Lebensm. Ing. Gabriela Haunschild (Südzucker AG, Mannheim) for providing physical data of sucrose.

5 References

Chapuliot, S., Gourdin, C., Payen, T., Magnaud, J.P., Monavon, A.: “Hydro-thermal-mechanical analysis of thermal fatigue in a mixing tee”, Nuclear Engineering and Design 235 (2005), 575-596.

Germano, M., Piomeli, U., Moin, P., Cabot, W.H.: "A dynamic subgrid-scale eddy viscosity model," Phys. Fluids, A 3, pp. 1760-1765 (1991).

Kapulla, R., Dyck, C., Witte, M., Fokken, J., and Leder, A. (2009), Optical flow and cross correlation techniques for velocity field calculation, Fachtagung “Lasermethoden in der Strömungsmesstechnik”, 8.–10. September 2009, Erlangen.

Metzner, K.J., Wilke, U.: “European THERFAT project – thermal fatigue evaluation of pip-ing system “Tee”-connections”, Nuclear Engineering and Design 235 (2005), 473-484.

Pope, S.B.: “Turbulent flows”, Cambridge University Press (2000).

Prasser, H.M., Böttger, A., Zschau, J.: "A new electrode-mesh tomograph for gas-liquid flows", Flow measurement and instrumentation,9 (1998), 111-119

Raffel, M., Willert, C., Wereley, S., Kompenhans, J., Particle Image Velocimetry: A Practical Guide, Springer, Berlin; Auflage: 2nd ed. (2007).

Walker, C., Simiano, M., Zboray, R., Prasser, H.M.: “Investigations on mixing phenomena in single-phase flow in a T-junction geometry”, Nuclear Engineering and Design 239 (2009), 116-126.